

The anatomy of tubercles: A corrosion study in a fresh water estuary

Dedicated to Professor Dr. Wolfgang Sand on the occasion of his 60th birthday

R. I. Ray, J. S. Lee, B. J. Little* and T. L. Gerke

The structure and mineralogy of corrosion products formed on carbon steel coupons exposed in Duluth Superior Harbor (DSH, USA), were investigated and compared with corrosion products on similar substrata from other locations. Corrosion products in DSH form within a few months each year and are removed by ice scour and reform. The corrosion products formed in DSH are tubercles with an outer surface, an inner shell of magnetite, and a core of iron(III) oxyhydroxides, goethite, and lepidocrocite, in association with stalks produced by bacteria. In general, the tubercles formed in DSH are similar in morphology and mineralogy to corrosion products described for carbon steel and cast iron exposed to treated waters in decades-old drinking water and cooling water systems. DSH tubercles are unique in several structural details. DSH tubercles increase areal coverage of the substratum by consolidation of tubercles. Furthermore, the core material extends into the pit and is an exact replica of the pit profile.

1 Introduction

The term tubercle, meaning a small rounded prominence, has been used to refer to iron corrosion products on steel surfaces exposed in treated (i.e., chlorinated and heated) fresh waters. *Herro* [1] working with iron corrosion products formed in cooling water systems, defined tubercles as structurally complex corrosion cells in which accumulations of metal oxides, deposits, and corrosion products cap localized regions of metal loss. He concluded that differential aeration cells caused tuberculation, suggesting that oxygen deficient regions below the accumulated corrosion products were anodic sites, while surrounding areas were cathodic. He indicated that tubercles grew as a result of both internal (anodic) and external (cathodic) reactions, i.e., anodic dissolution of metal resulted in the accumulation of iron(II) (ferrous) and iron(III) (ferric) ions and cathodic reactions outside the tubercle reduced the pH and caused the precipitation of carbonate and other species whose solubility decreases with

increasing pH. *Herro* [1] suggested that tubercle morphology depended on water chemistry, dissolved oxygen concentration, temperature, flow, and corrosion rates.

In contrast, *Gerke et al.* [2] described tubercles formed in a 90-year old chlorinated drinking water distribution system (DWDS) that were not associated with significant localized corrosion. Furthermore, the tubercles within a single DWDS, exposed to the same water had different structures and differing amounts of associated heavy metals. They proposed that parameters other than water quality could control tubercle formation and growth.

The role of microorganisms in tubercle formation is also controversial. Several investigators have demonstrated bacteria and bacterial stalks within tubercles [3–5]. *Tuovinen* and *Hsu* [6] suggested that there were zones within some tubercles that contained enough organic carbon and other nutrients to support the growth of microorganisms and microcosms with symbiotic relationships and nutrient cycling. *Miller* and *Tiller* [7] indicated, “iron bacteria, which, together with the ferric hydroxide they produce can form extensive deposits called tubercles on the inside of water pipes.” *Tiller* [4] suggested that iron-oxidizing bacteria “encouraged” the formation of tubercles. However, bacteria are not the only cause of tubercle development and the presence of tubercles cannot be used to conclude the involvement of bacteria or microbiologically influenced corrosion. *Menzies* [8] described abiotic tubercle formation at breaks or discontinuities in an oxide scale exposed in an oxygenated environment. “Anodic dissolution

R. I. Ray, J. S. Lee, B. J. Little

Naval Research Laboratory, Code 7303, Bldg. 1009, Stennis Space Center, MS 39529 (USA)

E-mail: blittle@nrlssc.navy.mil

T. L. Gerke

Department of Geology, University of Cincinnati, Cincinnati, OH 45221 (USA)

takes place and as metal ions concentrate in the solution the solubility product of the solid hydroxide is exceeded locally and hydroxide precipitates out as a hemispherical membrane which surrounds and covers the original discontinuity. This results in effective screening of the anodic area from available oxygen and the metal at the discontinuity remains anodic.” Tubercles have been reported in boilers where oxygen is dissolved in water at high pressures and temperatures exceeding 100 °C and in sulfuric acid baths.

Tubercles were recently identified in association with pitting on carbon steel pilings in Duluth Superior Harbor (DSH), MN and WI, a freshwater estuary [5]. Ray et al. [5] identified bacteria, bacterial stalks and iron, in addition to other heavy metals, within the DSH tubercles. Copper, isolated in a distinct stratum at the base of the tubercles, was the most abundant heavy metal (other than iron). They concluded that the aggressive corrosion in DSH was due to the galvanic couple between the deposited copper and the carbon steel pilings. DSH is icebound from mid-December to mid-April and during that time has a durable, well-defined ice cover. Freeze ice thicknesses in DSH range from 0.5 to 1.4 m in addition to snow ice, stack ice, and ice from wave and splash action along harbor walls. Ice scour breaks and removes tubercles each year and tubercles reform within a few months. Experiments described in this paper were designed to examine the structure, microbiology, and mineralogy of tubercles on carbon steel pilings in DSH. In addition the characteristics of the DSH tubercles were compared to tubercles of varying ages isolated from other freshwater environments.

2 Materials and Methods

Coupons of 0.9525 cm thick A328 (0.035% max P, 0.04% max S, and 0.20% min Cu) cold rolled sheet pile were cut to an average size of 19.3 cm × 11.6 cm and placed in holders at locations throughout DSH. Divers collected coupons annually (prior to ice formation) for three consecutive years. Details related to coupon

placement, retrieval, and shipping have been reported elsewhere [5]. Exposure locations are shown in Fig. 1. Coupons were imaged using a Nikon S-700 digital camera prior to and after cleaning with a solution of hydrochloric acid and distilled water (1:1) with 3.5 g/L of hexamethylene-tetramine [9]. Pit profiles (depth and area) were collected from five (25 mm × 25 mm) locations on each of three coupons every year using a Microphotronics Nanovea PS50 non-contact optical profiler with a 3.5 mm optical pen. Pit depth and area were used to calculate mass loss. Tubercles were removed from DSH coupons and embedded in epoxy resin and sectioned using a diamond blade, slow speed saw [5]. The cross-sections were imaged with a digital camera and the dimensions of the tubercles were recorded. Tubercles (not embedded) were examined using environmental scanning electron microscopy (ESEM) coupled with energy dispersive X-ray spectrometry (EDS) as previously described [5]. The mineralogy of the tubercles was analyzed using a Siemens D-500 automated diffractometer system using a Cu K α radiation at 30 mA and 40 kV. The 2 θ ranged from 5 to 60°, with a 0.02° step, and a 2 s count time at each step. Crystalline phase identifications were made on the basis of peak position and peak intensities using the American Mineralogist Crystal Structure Database, the Mineral Database, and the International Center for Diffraction Data 2002 PDF-2 (see the following link: <http://rruff.geo.arizona.edu/AMS/amcsd.php>, <http://webmineral.com/>).

3 Results

Well-formed tubercles were observed at all DSH exposure locations over a 3-year period. The surface area covered by individual tubercles increased each year [2 cm × 3 cm – year-1 (Fig. 2), 3 cm × 5 cm – year-2, and 6 cm × 10 cm – year-3]. Tubercle height, 2–5 mm (above the surface of the metal) however remained constant over the 3-year exposure period. The general internal morphology of these tubercles, regardless of age, consisted of a surface layer, overlying a hard shell layer that typically enclosed a core region.

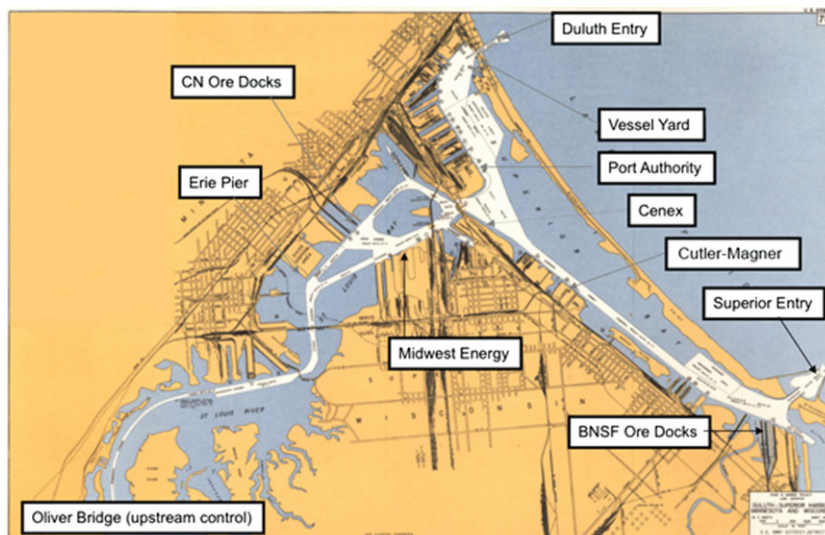


Figure 1. Map of the DSH with exposure locations



Figure 2. Tubercle on carbon steel after 1-year exposure in DSH

The surface layer of the DSH tubercles was made up of a reddish brown material composed of iron(III) oxyhydroxides, primarily goethite with trace amounts of lepidocrocite. A black hard shell that had both metallic and non-metallic luster under the surface layer was composed predominantly of magnetite with trace amounts of goethite and lepidocrocite. The core region, yellowish-brown in color and composed of goethite and lepidocrocite, extended into the area of localized corrosion (Fig. 3). The internal morphologies of the year-3 tubercles were a bit more complex in that they tended to contain multiple cores. In addition the cores had a fibrous appearance. ESEM imaging of the core regions demonstrated that the iron(III) oxyhydroxides were associated with twisted bacterial stalks (Fig. 4a and b). All DSH tubercles were associated with localized corrosion, i.e., pitting.

Pit volume, i.e., mass loss (depth \times area) increased with time over the 3-year exposure in all locations. Averaged pit volume data are shown for the Midwest Energy location (Fig. 5a–c). Acid cleaning of pre-exposed carbon steel coupons resulted in shallow pitting (metal loss) – 42.56 mm³ over 25 mm \times 25 mm (625 mm²) area (Fig. 5a). Pit volume for the year-1 coupon was typically 86.12 mm³ over 625 mm² with a range of pit depths (70–350 μ m)

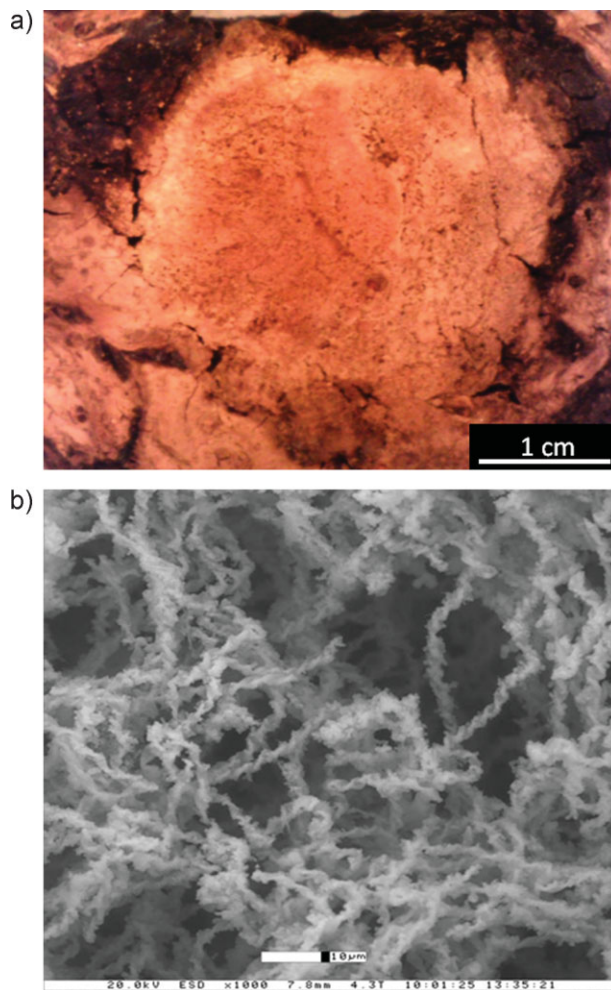


Figure 4. (a) Underside of tubercle core, showing black magnetite shell. (b) Twisted bacterial sheaths with deposited iron within tubercle core

(Fig. 5b). By year-3, the distribution of pit depths had increased (70–630 μ m) with a metal loss of 215.25 mm³ over 625 mm² (Fig. 5c). Pit depth varied among the locations (Table 1) and increase in pit depth with time was not linear. The deepest pits at

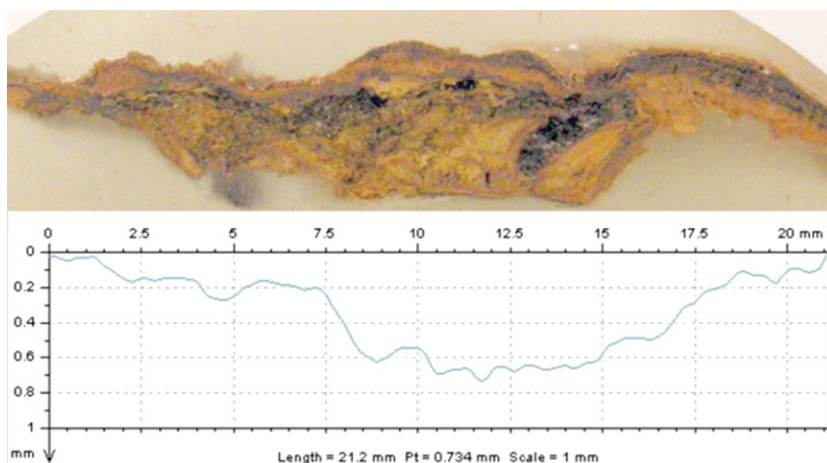


Figure 3. Year-3 tubercle with pit profile

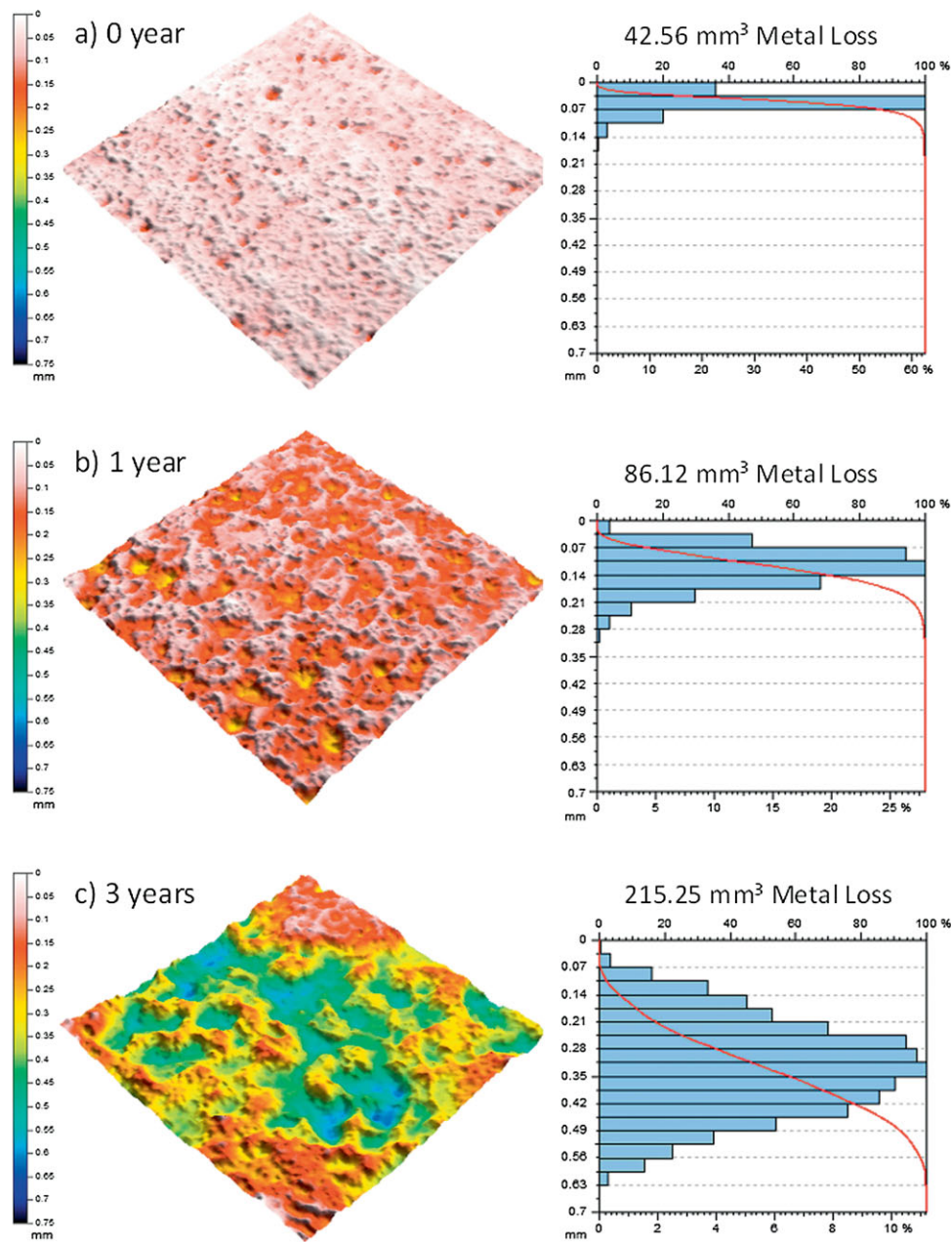


Figure 5. Three-dimensional representations, with accompanying pit density histograms, of carbon steel surfaces (625 mm²) exposed at Midwest Energy Dock illustrating increased pit depth and metal loss after acid cleaning; (a) prior to exposure, after (b) 1 year and (c) 3 years exposure

year-3 were measured in coupons collected from the Cutler–Magner location. Weight loss increased with time with an approximate 3–4% weight loss at all exposure sites after 3 years (Table 1).

4 Discussion

Carbon steel pilings in DSH that are over 30 years old are either completely or partially perforated by localized corrosion. Mass loss, a measure of general corrosion, for coupons exposed in DSH

was approximately 3–4% after 3 years. Average pit depth, a measure of localized corrosion in the year-3 coupons examined in this study, ranged between 670 and 788 μm , 7–8% of the total thickness of the coupons. Pit depth varied with location and increase in pit depth was not linear over the 3-year exposure. The rate of localized corrosion during the first year was faster than that measured in either of the next 2 years. *Sontheimer* et al. [10] found that corrosion of iron pipes occurred quickly during the first few years after placement into a DWDS and then slowed. However, the decrease in corrosion rate over time in a DWDS was influenced by the formation of an intact scale layer [11], a

Table 1. Compilation of corrosion data by location

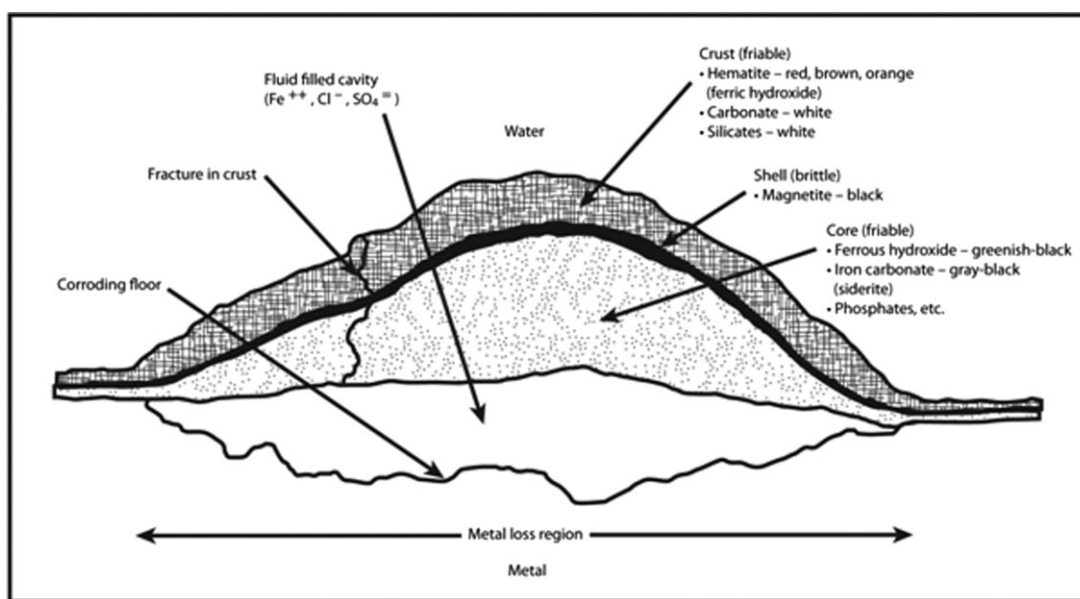
Location	Average pit depth (μm)			Weight loss (%)		
	10 months	Year-2	Year-3	Year-1	Year-2	Year-3
Oliver Bridge	445.8	469.5			2.4	
Hallett 7 Dock				0.9	2.1	
Hallett 5 Dock				1.1		3.8
Midwest Energy Dock	393.6	610.6	668.4	1.1	2.5	3.3
DSPA Berth 4			738.2	1.2	3.0	3.8
Cutler Magner	387.1		787.8	2.0	3.4	4.4

situation that does not apply to the ice-scoured pilings in DSH. In the absence of a better understanding of the relationship between water chemistry, tubercle formation, and corrosion, there are no scientific reasons to expect that the penetration rate will remain linear over decades.

Relative rates of tubercle growth could be evaluated by comparing the size of the DSH tubercles with those formed in other environments. The maximum DSH tubercle size after 3 years was 6 cm \times 10 cm. DSH tubercle height was remarkably similar for all three 3 years, approximately 2–5 mm. By comparison, tubercles from a 90-year old DWDS were approximately 4–6 cm in diameter and 2–3 cm high [2]. Tubercles formed in a few months each year in DSH were comparable in surface area to the undisturbed, older tubercles. Pit depth and height of the DSH tubercle above the surface of the metal were not related. DSH tubercle growth appears to include the possibility of merging tubercles as indicated by the multiple core regions after 3 years.

Several authors have described the internal morphologies of tubercles [1, 2, 12] and provided schematics of tubercles. *Herro* [1] indicated that tubercles should contain the following structural features: outer crust, inner shell, core material, fluid cavity, and corroding floor (Fig. 6). *Sarin* et al. [11, 12] indicated a surface

layer, a shell-like layer and a porous core over a corroding floor (Fig. 7). The significant difference between the *Herro* [1] and *Sarin* et al. [12] model is the absence of a fluid filled cavity in the *Sarin* et al. [12] model. Instead *Sarin* et al. [12] suggested that porosity within the tubercle determined the ease with which ions migrate within the core. Their diagram indicated increased porosity at the base of the core. *Gerke* et al. [2] examined the morphology, mineralogy, and chemistry of five tubercles from 90-year-old cast iron piping in a single DWDS. The overall morphology of all five DWDS samples was similar – a core with a hard shell layer, covered with surface material (Fig. 8). Magnetite, lepidocrocite, and goethite were the three predominant iron minerals in all five tubercles, but in different proportions. *Gerke* et al. [2] reported magnetite veins within core regions of some tubercles that produced a marbled appearance. They demonstrated that heavy metals were concentrated in regions of the tubercles. Tubercles exposed to the same water supply contained different metals or the same metals at different concentrations. The *Herro* [1] and *Gerke* et al. [2] schematics are similar in the following details: a magnetite shell overlain with a reddish brown crust, and a core. The fluid filled cavity between the core and the corroding floor, described by *Herro* [1], were not observed in the *Gerke* et al. [2] tubercles. *Gerke* et al. [2] indicated a core of either goethite or

**Figure 6.** *Herro* [1] schematic of tubercle

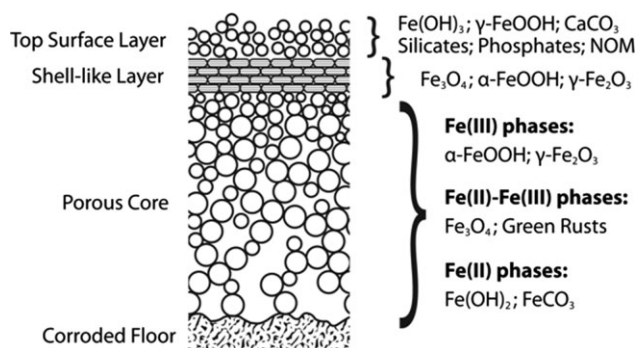


Figure 7. Sarin et al. [12] tubercle model

lepidocrocite and Herro [1] indicated a core of ferrous hydroxide, siderite, (iron carbonate) and phosphates. DSH tubercles are remarkably similar in area, general morphology and mineralogy to tubercles of varying ages from the three diverse sources. The previously published diagrams for the internal morphologies of tubercles however do not precisely describe the DSH tubercles. DSH tubercles have the following features: a crust, a shell, and a core. The core of DSH tubercles extends into the pit and is an exact replica of the pit interior. Figure 9 summarizes the information we have regarding the morphology and mineralogy of DSH tubercles.

The cores of DSH tubercles have fibrous textures composed of bacterial stalks and precipitated iron(III) oxyhydroxides. The previously cited authors [1, 2, 12] did not demonstrate bacteria within the tubercles they examined nor did they discuss a potential role for bacteria in tubercle formation. However, extracellular iron biomineralization has been studied extensively in fresh [13–16] and marine waters [17]. Chan et al. [18] concluded that polymer directed iron hydroxide mineralization is a general phenomenon that can occur in any system containing acidic polysaccharides and iron. Some iron-oxidizing microorganisms extrude polymeric structures upon which they deposit the ferric

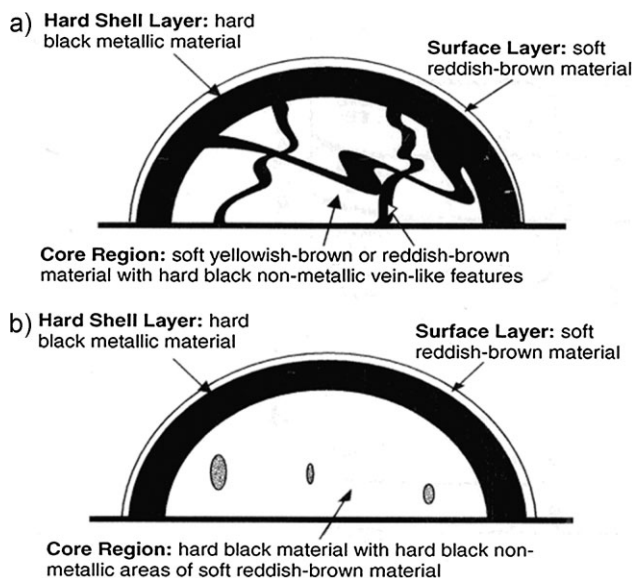


Figure 8. Gerke et al. [2] schematics of tubercles from DWDS

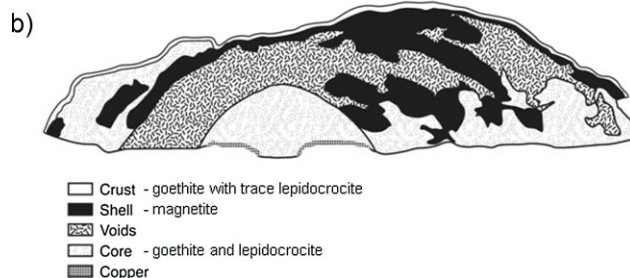


Figure 9. (a) Cross section of year-3 DSH tubercle. Scale in mm. (b) Schematic of DSH tubercle (a) with labels

iron derived from their metabolism. Banfield et al. [19] suggested that negatively charged polymers (e.g., *Gallionella* stalks) served as templates for aggregates of enzymatically produced iron oxides. Ghiorse and Ehrlich [20] suggested that microbial mineral formation can take place in intimate association with cells forming mineralized structures. They further concluded that the resulting structures could be used to identify a biological role in the mineral formation. Working with hyphal budding bacteria, Ghiorse and Hirsch [21] described the accumulation of positively charged iron hydroxides on negatively charged bacterial polymers. Once deposited, the iron oxides carried negative charges so that such a process could continue indefinitely without any biological activity. The only required biological input is the initial production of a negatively charged polymer. Sogaard et al. [22] described a similar process for biological iron precipitation by *Gallionella* in a polluted ground water (pH 5). Iron precipitated on the surface of the stalks until the negative charge effect was eliminated. The colloidal iron was condensed and the result was a dense deposit. Miot et al. [23] demonstrated precipitation of goethite on polymeric fibers extending from the cells of an iron-oxidizing bacterium. They also demonstrated a redox gradient, with the proportion of iron(III) highest near the cells and the proportion of iron(II) increasing at distance from the cell. Mineralized bacterial sheaths were observed in the core of DSH tubercles in association with iron(III)-rich oxides, i.e., goethite and lepidocrocite. Iron(II) rich magnetite was located at some distance from the core in the tubercle shell.

Another feature of DSH tubercles is the well-defined stratum of copper at the base of the tubercles that is the result of electrodeposition [5]. There is no direct relationship between the bacterial stalks in the core and the deposited copper. To date, there have been no other reports of distinct layers of copper associated

with iron tubercles. Sarin [11] reported the absorption of copper in iron corrosion scales. Gerke et al. [2] demonstrated that heavy metals, including copper, were either trapped within the structure or sorbed onto regions of the tubercles. In some tubercles the highest concentration of copper was located in the core region. Bacteriogenic iron oxides, formed in response to chemical or bacterial oxidation of iron(II) to iron(III), are made up of intact and/or partly degraded remains of bacterial cells mixed with amorphous hydrous iron(III) oxides [24]. Bacteriogenic iron oxides have reactive surfaces and act as sorbents of dissolved metal ions and enrichments of lead, cadmium, aluminum, chromium, zinc, manganese, and strontium, in addition to copper, have been reported [25, 26]. The relationship between sorbed metals and corrosion has not been investigated.

5 Conclusions

The presence of tubercles on carbon steel surfaces cannot be used as an indicator of localized corrosion. Tubercles are found in association with deep pitting and on surfaces with little or no pitting. The size, mineralogy, and morphology of iron corrosion products on carbon steel and cast iron surfaces from treated and untreated waters are remarkably similar, suggesting that formation is controlled by something other than water quality. In all cases the tubercles investigated and reviewed in this work were made up of a surface layer, shell, and core with the same general distribution of iron minerals. All DSH tubercles were associated with localized corrosion but the height of the tubercle above the surface cannot be used to predict pit depth under the tubercle. Bacterial stalks were located in the core regions of DSH tubercles. The findings of this study indicate that microorganisms may be important to the structure and mineralogy of tubercles on carbon steel formed in fresh water and that the mechanism(s) controlling the structure of iron corrosion products in chemically diverse fresh water environments may be similar.

Acknowledgements: This work was supported by the Office of Naval Research Program element 0601153N (6.1 Research Program) and the U.S. Army Corps of Engineers, Detroit District. NRL Publication number NRL/JA/7330-10-0254. We thank Timothy Phillips, Department of Geology, University of Cincinnati, for drafting Fig. 8.

6 References

- [1] H. M. Herro, presented at CORROSION/98 Paper 278, San Diego, CA, 1998.
- [2] T. L. Gerke, J. B. Maynard, M. R. Schock, D. L. Lytle, *Corros. Sci.* **2008**, *50*, 2030.
- [3] T. S. Rao, T. N. Sairam, B. Viswanathan, K. V. K. Nair, *Corros. Sci.* **2000**, *42*, 1417.
- [4] A. K. Tiller, in: R. N. Parkins (Ed.), *Corrosion Processes*, Applied Science Publishers, London and New York **1982**, 115.
- [5] R. I. Ray, J. S. Lee, B. J. Little, *Corrosion* **2009**, *65*, 707.
- [6] O. H. Tuovinen, J. C. Hsu, *Appl. Environ. Microbiol.* **1982**, *44*, 761.
- [7] J. D. A. Miller, A. K. Tiller, in: J. D. A. Miller (Ed.), *Microbial Aspects of Metallurgy*, American Elsevier Publishing Co., New York, **1970**, 61.
- [8] I. A. Menzies, in: J. D. A. Miller (Ed.), *Microbial Aspects of Metallurgy*, American Elsevier Publishing Co., New York, **1970**, 35.
- [9] ASTM International. *ASTM Standard G1-03, Vol. 3.02 Corrosion of Metals; Wear and Erosion* ASTM International, West Conshohocken, PA, **2003**.
- [10] H. Sontheimer, W. Kolle, V. L. Snoeyink, *J. Am. Water Works Assoc.* **1981**, *73*, 572.
- [11] P. Sarin, V. L. Snoeyink, J. Bebee, W. M. Kriven, J. A. Clement, *Water Res.* **2001**, *35*, 2961.
- [12] P. Sarin, V. L. Snoeyink, J. Bebee, K. K. Jim, M. A. Beckett, W. M. Kriven, J. A. Clement, *Water Res.* **2004**, *38*, 1259.
- [13] D. Fortin, S. Langley, A. Gault, A. Ibrahim, F. G. Ferris, I. D. Clark, *Geochim. Cosmochim. Acta* **2008**, *72*, A278.
- [14] R. E. James, F. G. Ferris, *Chem. Geol.* **2004**, *212*, 301.
- [15] C. S. Chan, G. De Stasio, S. A. Welch, M. Girasole, B. H. Frazer, M. V. Nesterova, S. Fakra, J. F. Banfield, *Science* **2004**, *303*, 1656.
- [16] L. St.-Cyr, D. Fortin, P. G. C. Campbell, *Aquat. Bot.* **1993**, *46*, 155.
- [17] C. T. S. Little, S. E. J. Glynn, R. A. Mills, *Geomicrobiol. J.* **2004**, *21*, 415.
- [18] C. S. Chan, S. C. Fakra, D. C. Edwards, D. Emerson, J. F. Banfield, *Geochim. Cosmochim. Acta* **2009**, *73*, 3807.
- [19] J. F. Banfield, S. A. Welch, H. Z. Zhang, T. T. Ebert, R. L. Penn, *Science* **2000**, *289*, 751.
- [20] W. C. Ghiorse, H. L. Ehrlich, in: H. C. W. Skinner, R. W. Fitzpatrick (Eds.), *Iron and Manganese Biomineralization Processes in Modern and Ancient Environments*, Catena Verlag, Cremlingen, Germany, **1992**, 75.
- [21] W. C. Ghiorse, P. Hirsch, *Arch. Microbiol.* **1979**, *123*, 213.
- [22] E. G. Sogaard, R. Aruna, J. Abraham-Peskir, C. B. Koch, *Appl. Geochem.* **2001**, *16*, 1129.
- [23] J. Miot, K. Benzerara, M. Obst, A. Kappler, F. Hegler, S. Schadler, C. Bouchez, F. Guyot, G. Morin, *Appl. Environ. Microbiol.* **2009**, *75*, 5586.
- [24] F. G. Ferris, *Geomicrobiol. J.* **2005**, *22*, 79.
- [25] D. Dong, X. Hua, Y. Li, J. Zhang, D. Yan, *Environ. Sci. Technol.* **2003**, *37*, 4106.
- [26] R. E. Martinez, F. G. Ferris, *Am. J. Sci.* **2005**, *305*, 854.

(Received: March 30, 2010)

W5739

(Accepted: April 22, 2010)